Novel wavelength-accurate InP-based arrayed waveguide grating*

Pan Pan(潘 盼), An Jun-Ming(安俊明)†, Wang Hong-Jie(王红杰), Wang Yue(王 玥), Zhang Jia-Shun(张家顺), Wang Liang-Liang(王亮亮), Dai Hong-Qing(代红庆), Zhang Xiao-Guang(张晓光), Wu Yuan-Da(吴远大), and Hu Xiong-Wei(胡雄伟)

State Key Laboratory on Integrated Optoelectronics, Institute of Semiconductors, Chinese Academy of Sciences, Beijing 100083, *China*

(Received 20 July 2013; revised manuscript received 11 September 2013; published online 10 February 2014)

A 13-channel, InP-based arrayed waveguide grating (AWG) is designed and fabricated in which the on-chip loss of the central channel is about −5 dB and the crosstalk is less than −23 dB in the center of the spectrum response. However, the central wavelength and channel spacing are deviated from the design values. To improve their accuracy, an optimized design is adopted to compensate the process error. As a result, the central wavelength 1549.9 nm and channel spacing 1.59 nm are obtained in the experiment, while their design values are 1549.32 nm and 1.6 nm, respectively. The route capability and thermo–optic characteristic of the AWG are also discussed in detail.

Keywords: arrayed waveguide grating, wavelength accuracy, thermo–optical characteristic, router

PACS: 42.82.Gw, 42.79.Sz, 42.82.Bq **DOI:** 10.1088/1674-1056/23/4/044210

1. Introduction

As indicted, total internet demand increases by about 40% per year, so greater transmission capacity is greatly required. Photonic integrated circuit (PIC) technology optimizes the manufacturing process by choosing a single material-InP with which it is possible to realize all of the necessary optical functions on a single semiconductor chip.[1] The transmitters and receivers in the terminal units of current wavelength-division multiplexing (WDM) systems operating at 1.3-μm or 1.55-μm wavelength are usually the devices based on InGaAsP epitaxial layers grown on InP substrates, which can satisfy the requirements of high-performance, low cost, and large scale.[2,3] PICs are of decisive importance for realizing a continuous rapid increase of the network, and a photonic network chip which is integrated with a complementary metal–oxide–semiconductor (CMOS) shows promise in overcoming limits on bandwidth and power faced by electrical interconnects. The Infinera Corporation is the pioneer in PIC technology, which has reported that more than 400 active and passive devices (lasers, modulators, photodetectors, switches, and so on) are integrated on one chip,[4] and in its next generation coherent 500-Gb/s PICs, over 600 optical functions are integrated into just two optical chips. PIC capabilities will continue to scale so that service providers can keep pace with the exponential growth in the network demand. As a multiplexer/demultiplexer, the arrayed waveguide grating (AWG) is the key component in WDM or the super-channel system. Silicon-based AWG[5] has been widely used in the planar lightwave circuit (PLC), which can be integrated with laser array in the transmitter and integrated with photodetectors in the receiver.[6,7] Although the multi-mode interferometer (MMI) can easily be integrated with laser array, the high loss makes it unusable in a practical application.[8] Many high-performance AWGs have been designed and fabricated for monolithic integration,[9,10] In this paper, a 13-channel InP-based AWG is designed and fabricated for a monolithic PIC, and the wavelength accuracy is optimized by improving the design values. Moreover, the route capability and thermo–optic characteristics of AWG are also discussed in detail.

2. Design and fabrication

2.1. Designed parameters

AWG consists of the input/output waveguides, input/output slabs, and arrayed waveguides. The input/output slabs are based on Rowland circle structure (The AWG is symmetric when the radii of the two Rowland circles are equal),[11] the symmetric AWG can be used as a multiplexer and a demultiplexer simultaneously. Table 1 shows the key parameters of the AWG. According to the parameters of calculation, we design the layout of the AWG. Figure 1 shows the schematic structure of the 13-channel InP-based AWG. The central wavelength and channel spacing are designed to be 1549.32 nm and 1.6 nm (200 GHz), respectively. The total effective dimension of the AWG is about 3.4 μm×4 μm.

*Project supported by the National High Technology Research and Development Program of China (Grant Nos. 2011AA010303 and 2013AA031401) and the National Natural Science Foundation of China (Grant No. 61090390).

†Corresponding author. E-mail: junming@semi.ac.cn

© 2014 Chinese Physical Society and IOP Publishing Ltd

Table 1. The key parameters of the AWG.

Parameter name	Value
Number of channels	5 in, 13 out
Number of arms	55
Waveguide width	2.6 μm
Etching depth	4.2 μm
Channel spacing ($\Delta\lambda$)	1.6 nm
Radius of Rowland circle (R)	1132.8 μm
Path-length difference (ΔL)	34.534 μm
Minimum bend radius	250 μm
Diffraction order (m)	73

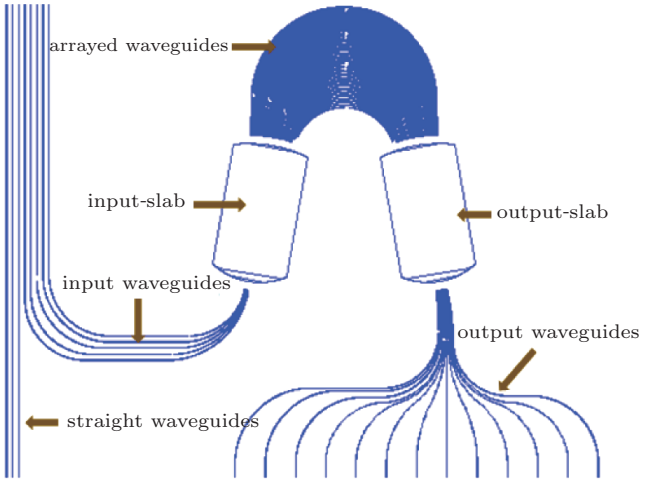


Fig. 1. (color online) Schematic structure of the 13-channel AWG.

2.2. Fabrication of device

For the fabrication of the device, firstly, a passive sandwich structure consisting of an InP substrate layer, an InGaAsP (1.05Q) core layer, and an InP cap layer was grown on the entire wafer by mental–organic chemical vapor deposition (MOCVD). Figure 2 shows the peak wavelength profile of the wafer, it can be seen that the minimum and maximum peak wavelengths are 1048.9 nm and 1053.2 nm, and in the center of the wafer, we have an average value of 1050.7 nm which is close to the designed value 1050 nm (1.05Q). Secondly, an SiO_2 layer was grown by plasma enhanced chemical vapor deposition (PECVD) as a hard mask, and a lithography step was used to transfer the AWG pattern on to the chip. Then the deep-ridge waveguide was formed by inductively coupled plasma (ICP) etching as shown in Fig. 3. From bottom to top, the different waveguide layers are a 1.6-μm InP substrate layer, a 0.5-μm InGaAsP core layer, a 1.5-μm InP cap layer, and the remaining SiO_2 hard mask which is about 700 nm. Finally, a 1-μm thick SiO_2 protecting layer was grown by PECVD to protect the device from external disturbance.

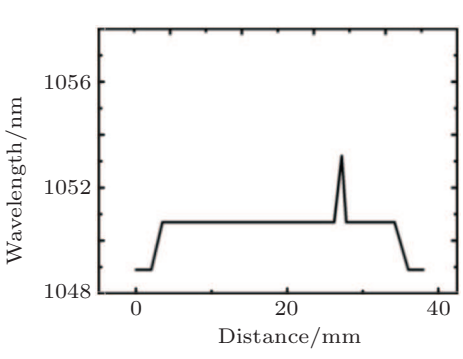


Fig. 2. Peak wavelength profile of the wafer.

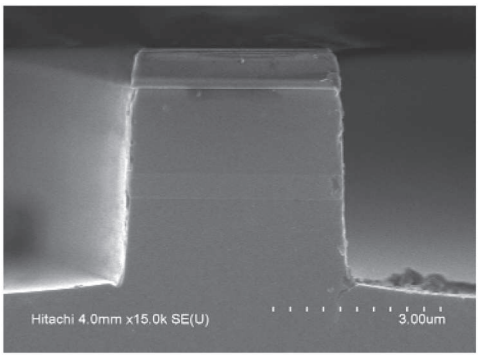


Fig. 3. Waveguide cross section.

3. Experimental results and analysis

3.1. Etching results of the waveguides

Figure 4(a) shows the etched side-walls of the arrayed waveguides, and the smooth side-walls result in low scattering loss. To decrease diffraction loss in the slabs, tapered waveguides are introduced in the junctions between slab

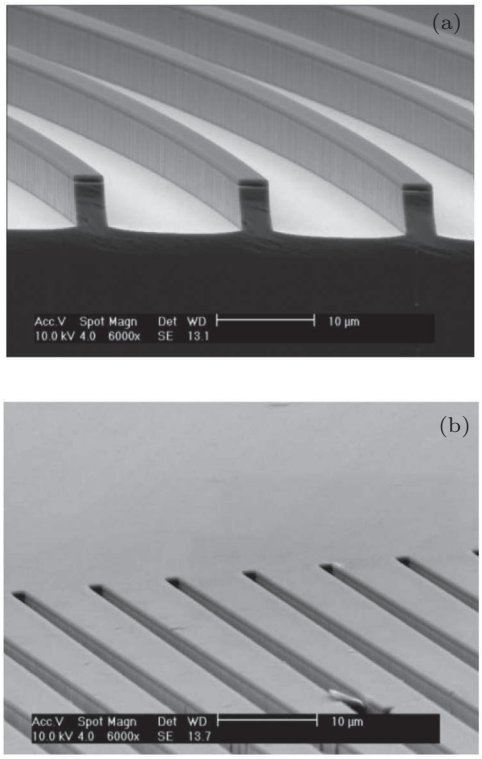


Fig. 4. Scanning electron micrograph (SEM) images of (a) the side-walls of arrayed waveguides and (b) the gaps between tapered waveguides.

waveguides and arrayed waveguides, so are between slab waveguides and input/output waveguides. These tapered waveguides are all 70-μm long and have widths ranging from 2.6 μm to 4.5 μm. Figure 4(b) shows the gaps between the tapered waveguides, and the minimum gap width is about 1 μm.

3.2. Measurement of fabricated AWG

The fabricated device is measured in our test platform, which consists of a broadband optical source, the optical fiber coupling system available from the Newport Company, a power meter and an optical spectrum analyser. Alignment coupling is a key technology in the test because of the small size of the device. A coupling efficiency of about 23% is obtained experimentally by adopting fused tapering fiber and horizontally tapered input/output waveguides. Similarly, with vertically tapered input/output waveguides and grating coupler the coupling loss is reduced, but the process difficulty is greatly increased.[12,13] The measured transmission spectra are shown in Fig. 5. The minimum on-chip loss at the central channel is about −5 dB, the channel non-uniformity is about 1.8 dB, and the crosstalk is less than −23 dB in the center of the spectrum response. The measured device has good performance in on-chip loss and crosstalk. However, the central wavelength 1555.2 nm and channel spacing 1.5 nm deviate from the designed values which are 1549.32 nm and 1.6 nm, respectively.

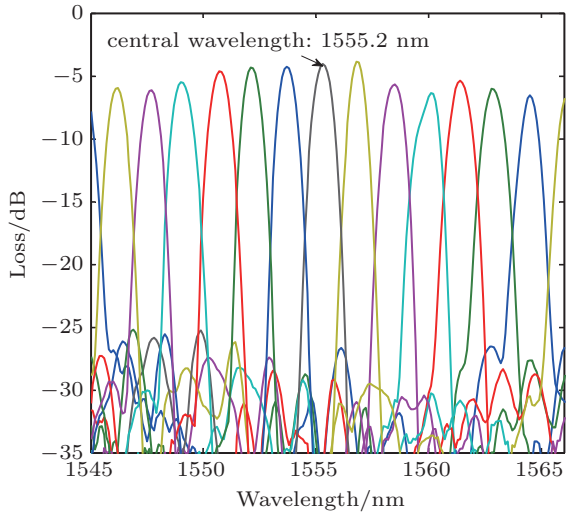


Fig. 5. (color online) Spectral response of the fabricated AWG.

3.3. Optimized design and results

After many experiments, we obtained stable process parameters that guarantee the uniformity in one wafer and repeatability in different wafers. As shown in Fig. 6, the central wavelengths of devices in the same wafer are nearly the same and the differences in wavelength among devices on different wafers are less than 0.15 nm. Because of the process stability, the better performance in the sense of wavelength accuracy can be obtained through tuning some design parameters. According to the design principle of AWG, we can obtain the grating diffraction equation that the AWG meets:

$$n_s d \sin\theta_i + n_s d \sin\theta_0 + n_c \Delta L = m\lambda, \tag{1}$$

where θ_i and θ_0 are the dispersion angles, m is the diffraction series, d is the separation distance between adjacent arrayed waveguides, ΔL is the length difference between adjacent arrayed waveguides, n_s and n_c are the effective indices of slab waveguide and arrayed waveguide, respectively. According to the angular dispersion relation of AWG, the relation between channel spacing $\Delta\lambda$ and dispersion angle $\Delta\theta$ can be expressed as follows:

$$\Delta\lambda = \Delta\theta \cdot \left(\frac{\mathrm{d}\theta}{\mathrm{d}\lambda}\right)^{-1} = \frac{\Delta x_0}{R} \cdot \frac{n_s d}{m} \cdot \frac{n_c}{n_g}, \tag{2}$$

where Δx_0 is the separation distance between adjacent input and output waveguides, R is the radius of the Rowland circle, and n_g is the group index. In addition, the length difference between the adjacent arrayed waveguide ΔL is related to the central wavelength λ_0, and the relationship can be written as

$$\Delta L = \frac{m\lambda_0}{n_c}. \tag{3}$$

According to formulas (2) and (3), the central wavelength λ_0 and the channel spacing $\Delta\lambda$ are influenced by ΔL and R respectively. λ_0 will be more accurate by adjusting ΔL from 34.534 μm to 31.990 μm and $\Delta\lambda$ can be adjusted by changing the radius of the Rowland circle R. As $\Delta\lambda \propto 1/R$, when $\Delta\lambda$ is changed from 1.5 nm to 1.6 nm, R will be changed from 1132.8 μm to 1144.47 μm. The optimized AWG is fabricated in the same process conditions. Figure 7 shows the spectra response of the improved device. The central wavelength is 1549.9 nm and the channel spacing is about 1.59 nm, which means that the values of the optimized AWG accord well with our design values. Meanwhile, the basic characteristics (insertion loss and crosstalk) practically have not been affected.

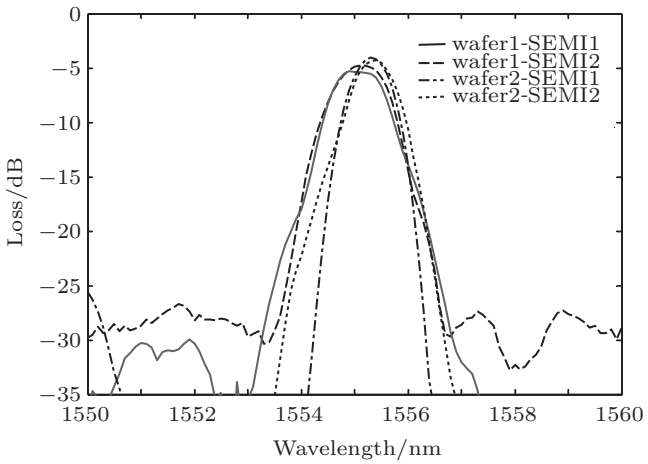


Fig. 6. Central wavelength spectra of different devices in one wafer and different wafers.

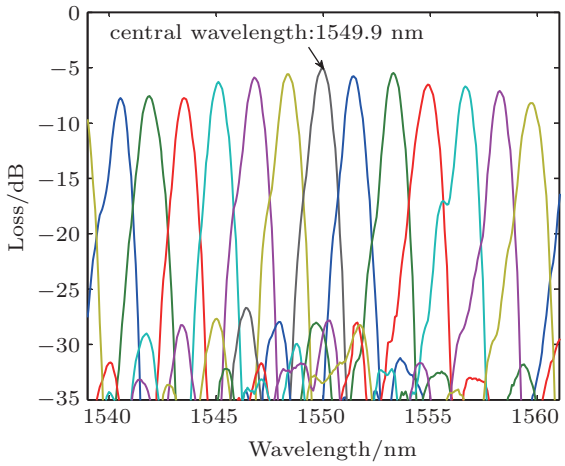


Fig. 7. (color online) Spectral response of the optimized AWG.

3.4. Thermo–optic characteristic for further wavelength fine-tuning

As wavelength stability in InP AWGs is very important when they are integrated with lasers and other active devices in building dense wavelength-division multiplexing (DWDM) optical networks, we investigate the AWG in different temperature conditions (ranging from 25 °C to 50 °C). The result in Fig. 8 shows that the device is temperature-sensitive, as the temperature is raised by 1 °C, the wavelength has a red shift of about 0.09 nm. The wavelength shift is mainly due to the thermo–optical characteristic of arrayed waveguides, and can be expressed as

$$\frac{\mathrm{d}n}{\mathrm{d}T}\cdot(\Delta L)=m\frac{\mathrm{d}\lambda_0}{\mathrm{d}T}, \tag{4}$$

where m is the diffraction order of the AWG.

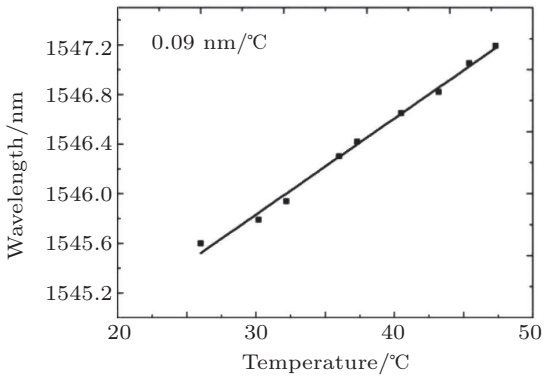


Fig. 8. Wavelength drift related to temperature.

From the above formula, we can infer that the temperature coefficient of the InP waveguide effective refractive index is 1.85×10^{-4}/°C which is very close to the calculated value.[14,15] As a fine tuning method, thermal tuning can be easily used in the InP-based AWG. We can use a Ti/W alloy as a thermode above the arrayed waveguides and aluminum as the lead wire. While inputting current, the thermode will change the refractive index of arrayed waveguides, so that the central wavelength shifts. The wavelength accuracy will be further optimized by thermal tuning.

3.5. AWG router

An $N\times N$ AWG router which shows good cyclic rotation property is a key unit in the PIC optical router, so we also design an AWG with good cyclic properties. If the free-spectrum range (FSR) of the $N\times N$ AWG is N times the channel spacing (N is the quantity of input/output channels), signals f_{i} and $f_{\mathrm{i}N}$ ($f_{\mathrm{i}N}=f_{\mathrm{i}}+\mathrm{FSR}$) would be output from the same output port if they are entered into the same input port. The AWG router with cyclic wavelength properties is not only used as a multiplexer and demultiplexer but also used for fabricating more complicated photonic devices such as an add-drop multiplexer[16] or a wavelength-selective switch.[17] Figure 9 shows that in an AWG with cyclic wavelength properties, marginal signal will not be dropped but output in the same output port with the signals whose wavelength difference is in an FSR. Route capability is an important characteristic of this AWG, which is verified by inputting signals in different input ports (input port 0 and 1). As shown in Fig. 10, the solid curves exhibit the spectra of signals input from input port 0, while the dashed curves exhibit the spectra of signals input from input port 1. Numbers in the solid-line box and dotted-line box above the spectral curves represent the different outputs when signal is input from input port 0 and input port 1, respectively. Signal f_{i} and $f_{\mathrm{i}N}$ ($f_{\mathrm{i}N}=f_{\mathrm{i}}+\mathrm{FSR}$) would be output from the same output port if they are entered into the same input port. Apparently, the marginal signal will not be dropped but output from the same output port with the signal whose wavelength difference is in an FSR. From Fig. 10 we also find some small errors between the two output spectra, which is mainly because the unstable testing environment and the fabrication error between the two different input waveguides.

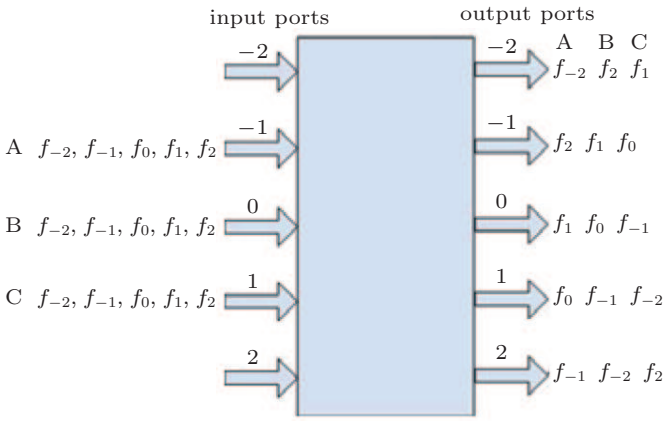


Fig. 9. (color online) The periodicity of AWG.

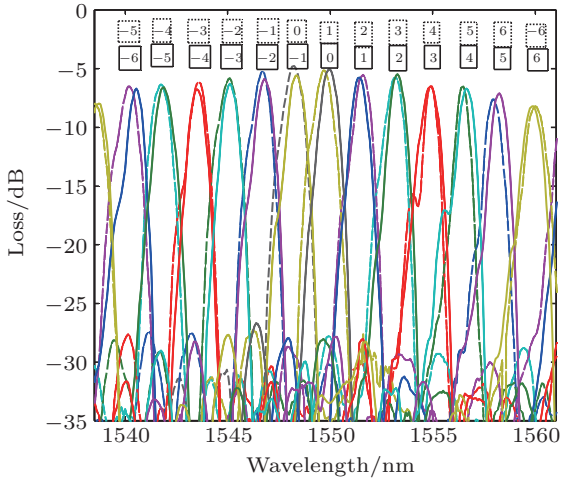


Fig. 10. (color online) Spectrum responses when signal is input from input port 0 (solid curves) and input port 1 (dashed curves), numbers in the box represent the output ports.

4. Conclusions

In this paper, we designed and fabricated a wavelength-accurate AWG and analyzed it experimentally and theoretically. The wavelength accuracy is improved by adjusting the designed values R and ΔL, and the central wavelength and average channel spacing are 1549.9 nm and 1.59 nm, respectively. Meanwhile, the on-chip loss of the central channel is about -5 dB and crosstalk is less than -23 dB. Testing of the thermal–optical characteristics shows that the wavelength is shifted by 0.09 nm when temperature is raised by 1 °C, so that thermal tuning is practicable in this AWG for fine tuning. This AWG is also designed with good route capability, i.e., the marginal signal is not dropped: it can be used for more complicated photonic devices such as an add-drop multiplexer or a wavelength-selective switch. This device is widely used in 100-Gb/s DWDM network system.

References

[1] Tolstikhin V I, Moore R, Pimenov K, Logvin Y, Wu F and Watson C D 2009 *European Conference on Optical Communication*, September 20, 2009, Vienna, Austria, p. 1

[2] Nagarajan R, Joyner C H, Schneider R P, Bostak J S, Butrie T, Dentai A G, Dominic V G, Evans P W, Kato M, Kauffman M, Lambert D J H, Mathis S K, Mathur A, Miles R H, Mitchell M L, Missey M J, Murthy S, Nilsson A C, Peters F H, Pennypacker S C, Pleumeekers J L, Salvatore R A, Schlenker R K, Taylor R B, Huan-Shang Tsai, Van Leeuwen M F, Webjorn J, Ziari M, Perkins D, Singh J, Grub S G, Reffle M S, Mehuys D G, Kish F A and Welch D F 2005 *IEEE J. Select. Topics Quantum Electron.* **11** 50

[3] Kish F A, Welch D, Nagarajan R, Pleumeekers J L, Lal V, Ziari M, Nilsson A, Kato M, Murthy S, Evans P, Corzine S W, Mitchell M, Samra P, Missey M, DeMars S, Schneider R P, Reffle M S, Butrie T, Rahn J T, Van Leeuwen M, Stewart J W, Lambert D J H, Muthiah R C, Huan-Shang Tsai, Bostak J S, Dentai A, Kuang-Tsan Wu, Han Sun, Pavinski D J, Jiaming Zhang, Jie Tang, McNicol J, Kuntz M, Dominic V, Taylor B D, Salvatore Randal A, Fisher M, Spannagel A, Strzelecka E, Studenkov P, Raburn M, Williams W, Christini D, Thomson K K, Agashe S S, Malendevich R, Goldfarb G, Melle S, Joyner C, Kaufman M and Grub S G 2011 *IEEE J. Select. Topics Quantum Electron.* **17** 1470

[4] Nagarajan R, Kato M, Dominic V G, Joyner C H, Schneider R P, Dentai A G, Desikan T, Evans P W, Kauffman M, Lambert D J H, Mathis S K, Mathur A, Mitchell M L, Missey M J, Murthy S, Nilsson A C, Peters F H, Pleumeekers J L, Salvatore R A, Taylor R B, Van Leeuwen M F, Webjorn J, Ziari M, Grubb S G, Perkins D, Reffle M, Mehuys D G, Kish F and Welch D 2005 *Electron. Lett.* **41** 347

[5] An J M, Wu Y D, Li J, Wang H J, Li J Y and Hu X W 2008 *Chin. Phys. Lett.* **25** 1717

[6] Nagarajan R, Kato M, Pleumeekers J, Evans P, Lambert D J H, Chen A, Dominic V, Mathur A, Chavarkar P, Missey M, Dentai A, Hurtt S, Bäck J, Muthiah R, Murthy S, Salvatore R, Joyner C, Rossi J, Schneider R, Ziari M, Tsai H S, Bostak J, Kauffman M, Pennypacker S, Butrie T, Reffle M, Mehuys D, Mitchell M, Nilsson A, Grubb S, Kish F and Welch D 2007 *J. Opt. Net.* **6** 102

[7] Soares F M, Fontaine N K, Scott R P, Baek J H, Zhou X, Su T, Cheng S, Wang Y, Junesand C, Lourdudoss S, Liou K Y, Hamm R A, Wang W, Patel B, Gruezke L A, Tsang W T, Heritage J P and Yoo S J B 2011 *IEEE Photon. J.* **3** 975

[8] Ma L, Zhu H L, Liang S, Zhao L J and Chen M H 2013 *Chin. Phys. B* **22** 054211

[9] Barbarin Y, Leijtens X J M, Bente E A J M, Louzao C M, Kooiman J R and Smit M K 2004 *Integrated Photonics Research,* June 30, 2004, San Francisco, California, USA, p. IThG4

[10] Baek J H, Soares F M, Seo S W, Jiang W, Fontaine N K and Broeke R G 2009 *IEEE Photon. Technol. Lett.* **21** 298

[11] Marz R and Cremer C 1992 *J. Lightwave Technol.* **10** 2017

[12] Sugita A, Kaneko A, Okamoto K, Itoh M, Himeno A and Ohmori Y 2000 *IEEE Photon. Technol. Lett.* **12** 1180

[13] Luyssaert B, Vanderateegen P, Taillaert D, Dumon P and Bogaerts W 2005 *IEEE Photon. Technol. Lett.* **17** 73

[14] Bertolotti M, Bogdanov V, Ferrari A, Jascow A, Nazorova N, Pikhtlm A and Schirone L 1990 *J. Opt. Soc. Am. B* **7** 918

[15] Martin P, Skouri E M, Chusseau L, Alibert C and Bissessur H 1995 *Appl. Phys. Lett.* **67** 881

[16] Tachikawa Y, Inoue Y, Ishii M and Nozawa T 1996 *J. Lightwave Technol.* **14** 977

[17] Suzuki S, Himeno A and Ishii M 1998 *J. Lightwave Technol.* **16** 650